Manoeuvring modelling and control design of autonomous vessels on inland waterways

Downloaded from: https://research.chalmers.se, 2025-03-27 04:37 UTC

Citation for the original published paper (version of record):
Zhang, C., Dhyani, A., Ringsberg, J. et al (2024). Manoeuvring modelling and control design of autonomous vessels on inland waterways. Proceedings of The ASME 2024 43rd International Conference on Ocean, Offshore and Arctic Engineering (OMAE 2024), 5A-2024. http://dx.doi.org/10.1115/OMAE2024-126580

N.B. When citing this work, cite the original published paper.

research.chalmers.se offers the possibility of retrieving research publications produced at Chalmers University of Technology. It covers all kind of research output: articles, dissertations, conference papers, reports etc. since 2004. research.chalmers.se is administrated and maintained by Chalmers Library

(article starts on next page)

Proceedings of the ASME 2024 43rd International Conference on Ocean, Offshore and Arctic Engineering
OMAE2024
June 9-14, 2024, Singapore, Singapore

OMAE2024-126580

MANOEUVRING MODELLING AND CONTROL DESIGN OF AUTONOMOUS VESSELS ON INLAND WATERWAYS

Chengqian Zhang
Department of Mechanics and Maritime Sciences, Chalmers University of Technology, Sweden

Abhishek Dhyani
Department of Maritime and Transport Technology, Delft University of Technology, The Netherlands

Jonas W. Ringsberg
Department of Mechanics and Maritime Sciences, Chalmers University of Technology, Sweden

Fabian Thies
Department of Mechanics and Maritime Sciences, Chalmers University of Technology, Sweden

Vasso Reppa
Department of Maritime and Transport Technology, Delft University of Technology, The Netherlands

Rudy R. Negenborn
Department of Maritime and Transport Technology, Delft University of Technology, The Netherlands

ABSTRACT

Autonomous inland shipping has great potential to enable intelligent and sustainable freight transport. At the same time, with the increasing traffic on confined waterways, ensuring safe operations of these autonomous inland vessels within limited operational spaces becomes imperative. This will require considering hydrodynamic effects during control design stages. This study presents a comprehensive analysis of an autonomous inland vessel's manoeuvrability and controller design. The ship's motions are modelled using an enhanced Manoeuvring Modelling Group (MMG) model to account for the hydrodynamic effects of inland waterways, including water depths, river currents, and bank effects. A verification study is conducted utilising a pusher-barge prototype model in shallow water to verify the model's accuracy. Through the implementation of a controller, a course-keeping study is conducted to assess the vessel's steering performance across various inland waterway scenarios, including sailing along river bends and waterway intersections. The results show that the manoeuvring model can generate fast and accurate vessel trajectory predictions. It is found that the proposed control technique proves effective in mitigating the confinement effects and countering disturbances caused by river currents, thereby ensuring efficient course-keeping suitable for the considered type of autonomous vessels on inland waterways.

Keywords: control design, inland waterways, manoeuvring prediction

1. INTRODUCTION

The European inland waterways, which extend over 41,000 kilometres of rivers and canals, form a complex transport network connecting 25 countries, numerous cities, and vital industrial regions. However, despite their extensive network, these waterways have been underutilised in the past decade, accounting for a mere 6% of the continent's inland freight transport [1], in contrast to the 77% dominated by road transport. Given the strict emissions regulations and road congestion issues within the European Union, enhancing the use of inland waterways could be a reliable and effective solution.

To construct competitive, intelligent waterborne transport networks, using advanced inland waterway vessels (IWVs) with clean energy and a high degree of automation or autonomy is an ideal solution for next-generation transport. However, to promote the production and implementation of autonomous IWVs, numerous issues must be considered from both the technical and legislative perspectives. A comprehensive analysis of ship design, perception, path planning, motion control, and potential social-technical issues is required [2]. Among them, an energy-efficient path, or voyage planning, is one of the key challenges to ensure that these vessels align with environmental sustainability objectives. To achieve this, it is essential to develop a holistic system capable of reflecting and optimising energy management during the dynamic operations of vessels. Such a system should encompass an energy performance prediction model [3], a manoeuvring model, control design and routing algorithms. Consequently, this study addresses the issues related to the manoeuvring and effective control of IVWs. These

Copyright © 2024 by ASME

are critical factors in the operational analysis of dynamic inland waterways.

Inland waterway transport is generally very safe as these vessels normally sail at a relatively low speed. However, the operation of IWVs in confined water faces limitations due to factors such as canal width, variations in water levels, and river currents [4,5]. Their operation and navigational environments are distinguished from those of marine vessels sailing on unconstrained deep waters. Water depth, and in particular the effect of shallow waters, significantly influences the motion and manoeuvrability of IWVs [6,7]. Furthermore, inland vessels need to navigate close to riverbanks frequently to make way for upcoming or passing vessels. This proximity to banks can present additional navigational challenges for these vessels. [8]. Consequently, detailed assessments must be conducted when applying the seagoing-ship-based prediction methods on IWVs.

Developing new test manoeuvres and procedures is essential to enhance the accuracy of predictions concerning the dynamics of IWVs [9]. In Zhang et al. [10], a new manoeuvring model was proposed by including these above-mentioned hydrodynamic impacts (shallow water and bank effects) into the classical Manoeuvring Modelling Group (MMG) model [11]. It can rapidly and accurately predict a vessel's motion response in confined waterways, capturing shallow water and bank effects. The modular nature of the model allows for easy customisation to test various control strategies, control systems, environmental load effects, and applications, or integration with an energy system model to evaluate the vessel energy performance during dynamic operation. A rudder control model was subsequently developed, followed by a coupled analysis that incorporated both bank and current effects. This analysis investigated the vessel's manoeuvring performance in counteracting these additional disturbances, thereby maintaining a predefined course and ensuring operational safety. However, the simulation was limited to straight waterways, and the heading control employed was relatively simplistic, suitable only for navigating straight courses.

Hence, the aim of this study is to introduce an improved manoeuvring simulation model and controller design. This will facilitate the simulation and analysis of a virtual autonomous vessel's steering performance. The ship's motions were modelled using an enhanced MMG model [10] to calculate the hydrodynamic effects of inland waterways, including water depths, river currents, and bank effects. A course-keeping study is presented using a pusher-barge model to assess the vessel's steering capabilities in diverse and complex inland waterway situations, such as navigating river bends and intersections.

2. MANOEUVRING MODEL

Since IWVs normally sail in a relatively calm environment and are not frequently subjected to ocean waves, their vertical motions are minor and, thus, often neglected. Consequently, the manoeuvring model in this study focuses on solving the motion equations in three degrees of freedom (3-DoF), including surge, sway, and yaw motions.

Figure 1 presents the coordinate systems used. The IWV in twin propeller configuration operates in the earth-fixed coordinate system $(o_0 - x_0 y_0 z_0)$, and $(o - xyz)$ is the body-fixed coordinate system at the mid-ship. The centre of gravity (CoG) is located at $(x_G, 0, 0)$, ψ denotes the heading angle, δ is the rudder angle, and u and v represent the surge and sway velocities, respectively.

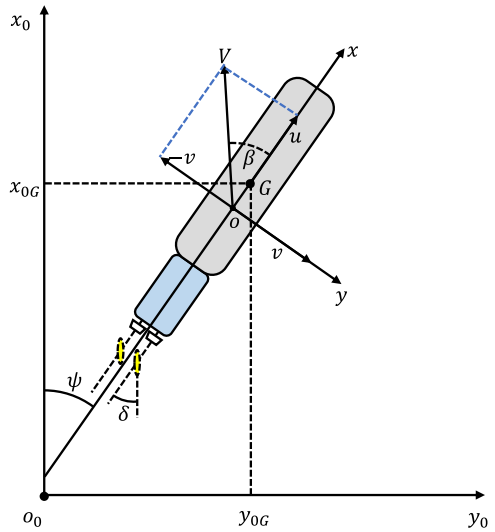

Figure 1: COORDINATE SYSTEM OF IWVs IN THIS STUDY.

2.1. Equations of motion

The MMG model was employed as the benchmark for predicting the motions of IWVs. This model features a modular architecture, decomposing the hydrodynamic forces and moments acting on the ship into individual components, including the hull, propeller, and rudder. This approach enables the analysis of ship motions by solving and quantifying the effects of these separate elements.

The original MMG model was designed for conventional sea-going vessels, which differ significantly from IWVs regarding hull shape, propeller-rudder configuration, and sailing conditions. A new manoeuvring model was proposed to enhance its applicability to inland waterways, particularly in confined environments. This model is a modification of the MMG model and includes additional considerations for shallow water and bank effects [10]. The equations of motion are formulated as:

$$\left.\begin{aligned} (m+m_x)\dot{u} - (m+m_y)v_m r - x_G m r^2 &= X_H + X_P + X_R + X_B \\ (m+m_x)\dot{v}_m - (m+m_x)ur + x_G m\dot{r} &= Y_H + Y_R + Y_B \\ (I_z + x_G^2 m + J_Z)\dot{r} + x_G m(\dot{v}_m + ur) &= N_H + N_R + N_B \end{aligned}\right\} \quad (1)$$

where the left-hand side represents the inertia terms, including the ship's mass (m), the added mass in the x- and y-directions $(m_x,\ m_y)$, the moment of inertia (I_z), and the added moment of inertia for yaw motion (J_z). The right-hand side terms (X, Y, N) denote the summation of the surge force, the sway force, and the yaw moment. The subscripts $H, P, R,$ and B represent the individual components from the ship hull, the propeller, the rudder, and the bank effect, respectively.

Copyright © 2024 by ASME

2.2. Hull forces and hydrodynamic derivatives

The hydrodynamic forces acting on the ship hull are formulated as:

$$\left.\begin{aligned} X_H &= 0.5\rho LTV^2 X'_H \\ Y_H &= 0.5\rho LTV^2 Y'_H \\ N_H &= 0.5\rho L^2 TV^2 N'_H \end{aligned}\right\} \quad (2)$$

where ρ is the freshwater density, L is the ship length, T is the draught, V is the vessel speed, and X'_H, Y'_H, N'_H represent the non-dimensional surge force, sway force, and yaw moment, which can be expressed as:

$$\left.\begin{aligned} X'_H &= -R'_0 \cos^2\beta_m + X'_{\beta\beta}\beta_m^2 + X'_{\beta r}\beta_m r' \\ &\quad + X'_{rr}r'^2 + X'_{\beta\beta\beta\beta}\beta_m^4 \\ Y'_H &= Y'_\beta\beta_m + Y'_r r' + Y'_{\beta\beta\beta}\beta_m^3 + Y'_{\beta\beta r}\beta_m^2 r' \\ &\quad + Y'_{\beta rr}\beta_m r'^2 + Y'_{rrr}r'^3 \\ N'_H &= N'_\beta\beta_m + N'_r r' + N'_{\beta\beta\beta}\beta_m^3 + N'_{\beta\beta r}\beta_m^2 r' \\ &\quad + N'_{\beta rr}\beta_m r'^2 + N'_{rrr}r'^3 \end{aligned}\right\} \quad (3)$$

where $X'_{\beta\beta}$, $X'_{\beta r}$, …, N'_{rrr} are the hydrodynamic derivatives. In Eq. (3), β_m is the mid-ship drift angle and r' is the non-dimensional yaw rate, and they can be computed by:

$$\begin{aligned} \beta_m &= -\tan^{-1}(v_m/u) \\ r' &= rL/V \end{aligned} \quad (4)$$

Eq. (5) presents the expression for the resistance coefficient, R'_0, which includes the shallow water effect using the method proposed in [3]:

$$\begin{aligned} R'_0 &= \frac{R_{Shallow}}{(0.5\rho LTV^2)} \\ R_{Shallow} &= 0.5\rho S_W U^2\left(C_F\left(1+(k+\Delta k)\right)+C_W\right) \end{aligned} \quad (5)$$

where Δk is the additional form factor [12] in shallow water based on the ratio of water depth (H) to ship draught (T). It can be computed as:

$$\Delta k = 0.644\left(\frac{H}{T}\right)^{-1.72} \quad (6)$$

2.3. Propeller force

IWVs are commonly equipped with twin propellers, ensuring sufficient thrust in shallow water conditions. The force generated by a twin propeller configuration is computed as:

$$X_P = (1-t)(T_P^P + T_P^S) \quad (7)$$

where t is the thrust deduction factor, and T_P^P and T_P^S represent the trust force delivered by the portside and starboard propellers, respectively. In this study, in terms of model simplification, it was assumed that the thrust force is identical for each propeller. This assumption is due to the complexity of accurately analysing the asymmetrical flow around twin propellers, particularly during steering manoeuvrers. Such an analysis requires experimental measurements of the flow field or detailed Computational Fluid Dynamics (CFD) simulations, which are beyond this model's development scope. In the Eq. (7), the thrust force is defined as:

$$T_P^P = T_P^S = \rho n_P^2 D_P^4 K_T(J) \quad (8)$$

where $K_T(J)$ is the thrust coefficient determined by the advance ratio J:

$$\begin{aligned} J &= u(1-w_P)/(n_P D_P) \\ w_P/w_{P0} &= \exp(-4\beta_P^2) \end{aligned} \quad (9)$$

where w_P is the wake fraction during ship steering. It is determined by the wake fraction for straight moving w_{P0} and propeller inflow angle β_P.

2.4. Rudder force

Contemporary IWVs are often equipped with multiple rudders to generate enough steering force. Given the complexity and uncertainty in modelling the flow behaviour of multiple rudders during steering, it was assumed (for simplification purposes) that each rudder's force and inflow angle were consistent. The rudder forces can be expressed by:

$$\left.\begin{aligned} X_R &= -(1-t_R)(F_N^P + F_N^S)\sin\delta \\ Y_R &= -(1+\alpha_H)(F_N^P + F_N^S)\cos\delta \\ N_R &= -(x_R + \alpha_H x_H)(F_N^P + F_N^S)\cos\delta \end{aligned}\right\} \quad (10)$$

where t_R is the steering resistance deduction factor, α_H represents the rudder force increase factor, x_R is the relative longitudinal coordinate of the rudder, and x_H is the longitudinal coordinate of the location at which the additional lateral force is acting. The terms F_N^P and F_N^S denote the summation of the rudder's normal force at each side. These factors are normally obtained from the experiments. Thus, the model's test results of a pusher barge convoy [6] were used as the input in this study.

2.5. Bank effect

IWVs navigate in restricted waterways. Due to the dynamic traffic on fairways, an IWV must frequently sail close to one side of the river or the canal banks to clear the way for other upcoming or passing vessels. The proximity of hull to channel wall can cause acceleration of the flow through the gap, leading to a pressure differential between the starboard and port sides. This will induce additional hydrodynamic force acting on the hull, which may affect the ship's course stability, also known as the bank effect.

To capture the characteristics of inland waterways, the model from [13] was introduced to capture the effects from the bank effect for various speeds, water depths, and ship-bank distances. The model is presented in Eq. (11) where the superscripts H, P, and HP denote the individual effects of pure speed (hull), propulsion, and coupled effect, Fr is the Froude number, and V_T is the reference velocity. α_{ik}^H, β_{ik}^H, α_{ik}^P, β_{ik}^P, α_{ik}^{HP}, and β_{ik}^{HP} are the regression coefficients from model tests; these parameters can be found in Vantorre's study [13]. It can be seen in Eq. (11) that the hydrodynamic effect of the bank is decomposed into individual factors, which can be easily incorporated into the modified MMG model.

Copyright © 2024 by ASME

$$
\left.
\begin{aligned}
Y_B^H &= 0.5\rho LTu^2 \sum_{i=1}^{2}\sum_{k=0}^{2} a_{ik}^H y_B^i \left(\frac{T}{H-T}\right)^k \\
N_B^H &= 0.5\rho L^2 Tu^2 \sum_{i=1}^{2}\sum_{k=0}^{2} \beta_{ik}^H y_B^i \left(\frac{T}{H-T}\right)^k \\
Y_B^P &= 0.5\rho LTV_T^2 \sum_{i=1}^{2}\sum_{k=0}^{2} a_{ik}^P y_B^i \left(\frac{T}{H-T}\right)^k \\
N_B^P &= 0.5\rho L^2 TV_T^2 \sum_{i=1}^{2}\sum_{k=0}^{2} \beta_{ik}^P y_B^i \left(\frac{T}{H-T}\right)^k \\
Y_B^{HP} &= 0.5\rho LTV_T^2 Fr \sum_{i=1}^{2}\sum_{k=0}^{2} a_{ik}^{HP} y_B^i \left(\frac{T}{H-T}\right)^k \\
N_B^{HP} &= 0.5\rho L^2 TV_T^2 Fr \sum_{i=1}^{2}\sum_{k=0}^{2} \beta_{ik}^{HP} y_B^i \left(\frac{T}{H-T}\right)^k
\end{aligned}
\right\} \quad (11)
$$

3. HEADING CONTROL

In contrast to seagoing vessels, the navigation environment for IWVs is more restricted due to the inherent limitations of waterways. Factors such as shallow waters, variable currents, and the bank effect can significantly affect the vessel's handling, thereby complicating course-keeping tasks. Consequently, precise heading control is crucial for safe navigation through narrow and curved waterways, avoiding collisions with banks or other obstacles. To facilitate this, the vessel's guidance system must generate an optimal trajectory from its current state to a designated point on the predefined path. Figure 2 presents a visualisation to describe this process of trajectory generation, where the corresponding waypoints, the desired trajectory, and the tracked trajectory for these scenarios are showcased here. The overall aim is to make the vessel's heading aligned with the predefined track. The desired heading $\psi(desired)$ is therefore containing a reference heading angle $\Delta\psi(WPT)$ between two consecutive waypoints (WPT_k, WPT_{k+1}), and a heading angle $\Delta\psi(cross)$ to reduce the cross-track error Δy:

$$\Delta\psi(cross) = -\tan^{-1}(\Delta y / X_D) \quad (12)$$

where X_D is a predefined reaction distance of the IWV, which has a length equal to 80 metres in this study.

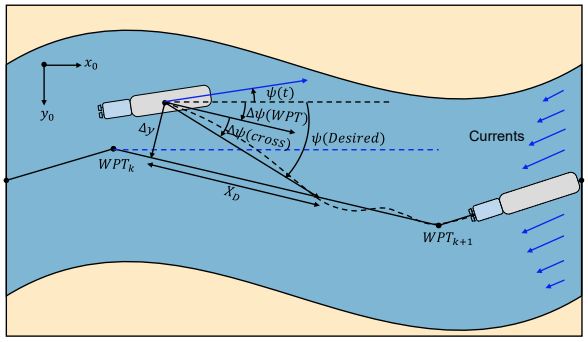

Figure 2: TRAJECTORY GENERATION FOR THE IWV HEADING CONTROL SCHEME.

3.1. Control design

The control design involves computing the commanded rudder angle δ_c to manipulate the vessel's position. A Proportional-Integral-Derivative (PID) reference tracking control law was designed to update δ_c at each time step:

$$\delta_{c_t} = K_p\left(\psi_{e_t} + T_d\left(\psi_{e_t} - \psi_{e_{t-1}}\right) + \frac{1}{T_i}\left(\sum_{k=0}^{t}\psi_{e_k}\right)\right) \quad (13)$$

where, ψ_{e_t} represents the error in the heading angle at the time step t. K_p is the controller's proportional gain, and T_d and T_i are the derivative and integral time constants, respectively. The Ziegler-Nichols method [14] was employed to select the optimal controller parameters, such that the heading error can be minimised. Furthermore, the vessel's speed was assumed to be constant throughout the heading control implementation. Figure 3 shows a block diagram schematic of the resulting closed-loop system.

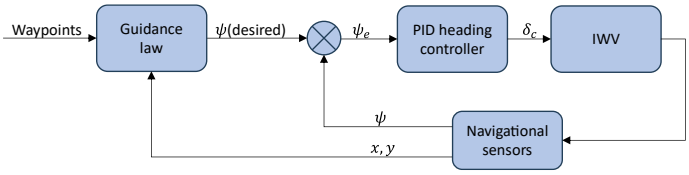

Figure 3: A SCHEMATIC OF THE CLOSED-LOOP SYSTEM FOR THE HEADING CONTROL OF THE IWV.

3.2. River currents

IWVs often face variable currents, particularly in river systems. Currents can make manoeuvring more complex, especially for those river systems with tight bends and narrow channels. To investigate the performance of the rudder controller under such scenarios, the influence of river currents was modelled by using reference ship speeds u_r and v_r [15] as:

$$\begin{aligned} u_r &= u - U_C\cos(\beta_C - \psi) \\ v_r &= v - U_C\sin(\beta_C - \psi) \end{aligned} \quad (14)$$

where β_C is the angle of incoming currents in the earth-fixed coordinate system. According to Duan [16], the current direction aligns with the tangential direction of the waterway, and the change of current velocity across a river follows a parabolic shape, meaning that the current has its maximum speed at the waterway centre (in this study, $U_{C_{MAX}} = 0.75$ m/s in all simulations) and decreasing to zero speed near the banks. It is important to note that in this study, the waterway was presumed to have a constant depth, represented by a rectangular cross-section. Consequently, the differences in current speed between the inside and the outside of a river bend, typically resulting from variations in depth, were not considered.

4. RESULTS

This section presents results from a verification of the manoeuvring model and the heading control simulations. The simulation study also serves the purpose of evaluating the controller's tracking performance and robustness. The control scenarios cover two typical tasks during the daily operations of

Copyright © 2024 by ASME

an IWV in inland waterways: course-keeping along river bends and steering at waterway confluence (intersections).

4.1. Model verification

The accuracy of the manoeuvring model must be checked before implementing the rudder controller. This study used the parameters of a pusher-barge model in Koh and Yasukawa [6]. The vessel's dimensions (see Table 1) and its hydrodynamic coefficients (see Table 2) were used as input in this study. The turning test was conducted for the rudder angles δ = 20° and δ = 35° with the ship speed U = 0.364 m/s (5 knots in full-scale).

Table 1: PUSHER-BARGE CONVOY PARAMETERS.

Parameter	Pusher	Barge	Pusher-barge
Length, L [m]	40.00	60.96	100.96
Ship Beam, B [m]	9.00	10.67	10.67
Draught, T [m]	2.20	2.74	2.74
Volume, ∇ [m^3]	494.7	1646.2	2140.9
Block coefficient, C_B [-]	0.633	0.924	0.725

Table 2: HYDRODYNAMIC COEFFICIENTS OF THE PUSHER-BARGE MODEL.

Symbol	Value	Symbol	Value
$X'_{\beta\beta}$	−0.3637	N'_{β}	0.4435
X'_{rr}	0.1055	N'_{r}	−0.0861
$X'_{\beta r}$	−0.248	$N'_{\beta\beta\beta}$	1.1277
Y'_{β}	1.2375	$N'_{\beta\beta r}$	−0.2249
Y'_{r}	−0.113	$N'_{\beta rr}$	−0.0561
$Y'_{\beta\beta\beta}$	4.2245	N'_{rrr}	−0.0522
$Y'_{\beta\beta r}$	3.6005	m'_{x}	0.0195
$Y'_{\beta rr}$	0.7129	m'_{y}	0.3722
Y'_{rrr}	−0.2003		

Figure 4 shows a comparison between the simulation results and literature data in full-scale at shallow water conditions ($H/T = 1.2$). It shows that using the hydrodynamic derivatives and vessel dimensions as the input, the manoeuvring model can correctly capture the vessel's turning behaviour.

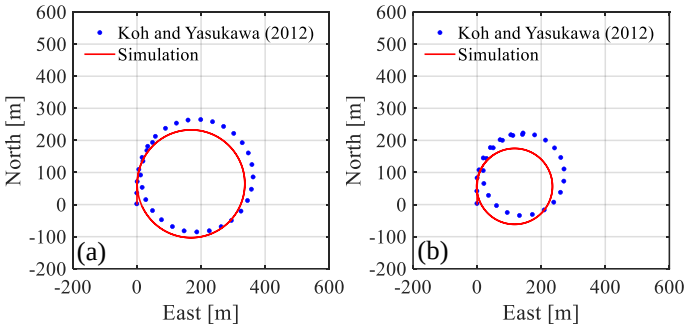

Figure 4: MODEL VERIFICATION ON TURNING: (a) δ = 35°, AND (b) δ = 20°.

4.2. Heading control for mid-channel sailing

The first operational condition is to maintain the IWV's course aligning with the waterway centreline, affording the vessel more room for manoeuvre with minimal bank effect. The IWV maintains a constant propulsion speed of 150 rpm, thus the ship speed over ground U_{SOG} varies according to its position along the river bend and the direction of the current, as shown in Figure 5. The ship encounters the maximum current speed at the waterway centre, resulting in a noticeably higher downstream speed. This allows the vessel to navigate the defined river bends in almost half the time it takes under upstream conditions.

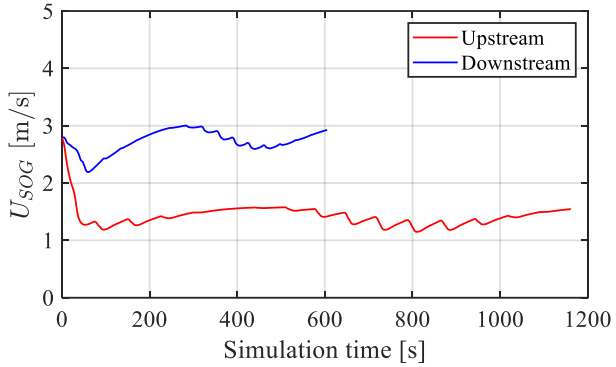

Figure 5: TIME HISTORIES OF THE U_{SOG} OF MID-CHANNEL SAILING

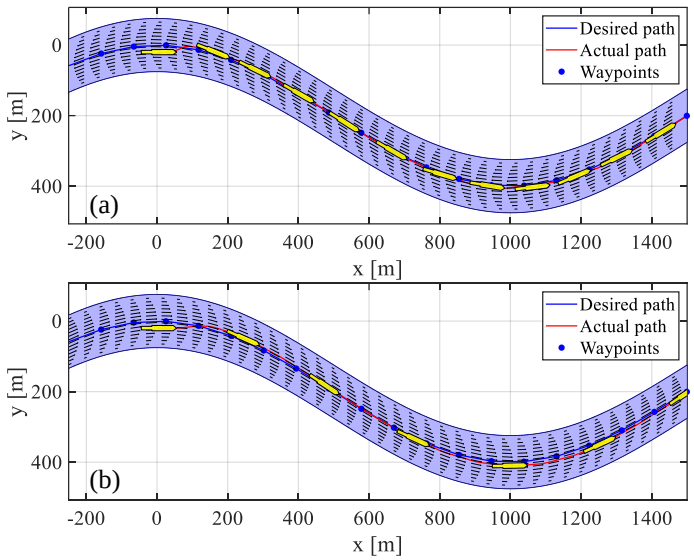

Figure 6: IWV TRAJECTORY OF MID-CHANNEL SAILING: (a) UPSTREAM CURRENT, AND (b) DOWNSTREAM CURRENT.

Figure 6 presents the IWV's trajectory under varying current directions, maintaining a constant propulsion speed of 150 rpm. The trajectory shows that with an oncoming current, the vessel achieves the desired path in a shorter distance compared to when it is sailing downstream. This is attributed to the rudders encountering a higher inflow speed, thus generating a greater steering force for course correction. In the second river bend,

Copyright © 2024 by ASME

approximately between 800 m and 1200 m, the IWV can rapidly adjust its heading to align with the predefined waypoints during upstream sailing. In contrast, downstream currents require a longer distance to manoeuvre the IWV effectively, as shown in Figure 6(b).

4.3. Heading control for sailing along banks

IWVs must frequently sail close to one side of the river or the canal banks to allow safe passage for other upcoming or overtaking vessels, particularly in narrow fairways. Under these conditions, the decreased ship-bank distance can cause additional hydrodynamic effects, which might impact the ship's handling. Therefore, effective rudder control is needed to counteract such effects in maintaining the desired course.

Under a same propulsion speed as before, the influence of current on ship speed will be decreased of near-bank sailing close to the right bank, for a ship-bank distance of 35 m, as shown in Figure 7. The time histories of side force acting on ships are present in Figure 8, where the rudder control effectively counteract the side force resulted from drifting and bank effect.

The corresponding trajectories under different current directions are shown in Figure 9. Compared to mid-channel sailing, the vessel's trajectory is significantly affected by an apparent bow-out moment and requires a longer distance to reach the predefined path when near a bank, particularly under a downstream current. However, once the vessel realigns with the desired course, the proposed controller effectively performs course-keeping in both scenarios.

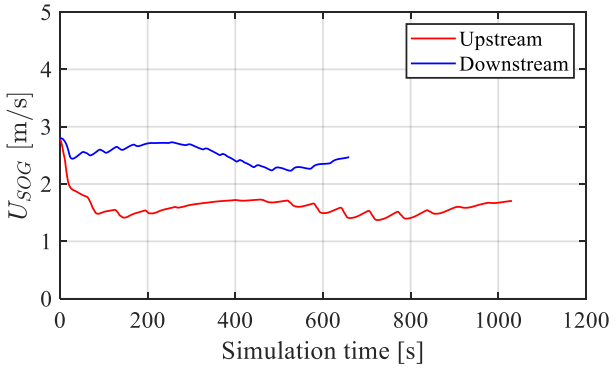

Figure 7: TIME HISTORIES OF THE U_{SOG} FROM SAILING ALONG THE RIGHT BANK.

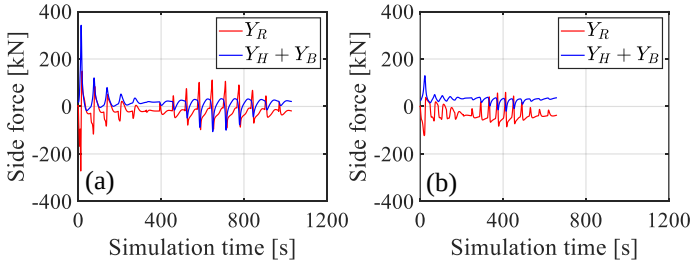

Figure 8: TIME HISTORIES OF SIDE FORCE (a) UPSTREAM CURRENT, AND (b) DOWNSTREAM CURRENT.

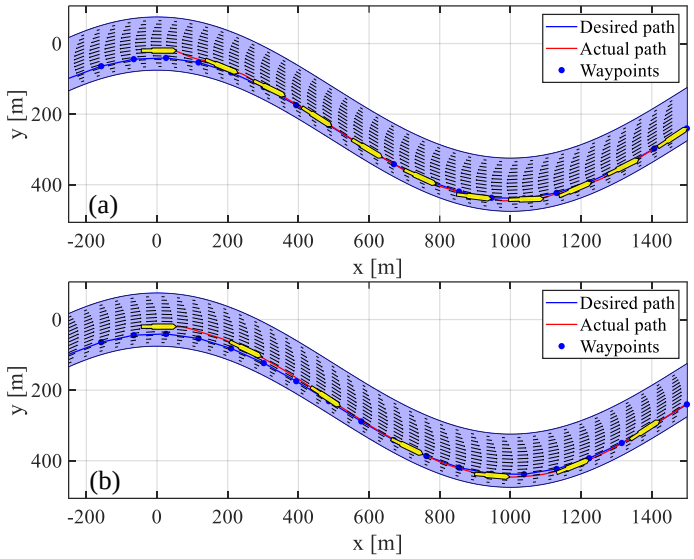

Figure 9: IWV TRAJECTORY FROM SAILING ALONG THE RIGHT BANK WITH A SHIP-BANK DISTANCE OF 35 METRES: (a) UPSTREAM CURRENT, AND (b) DOWNSTREAM CURRENT.

The trajectories show that the designed PID rudder controller is generally effective in adjusting the vessel's heading and minimising the cross-track error, particularly when navigating in river bends, as illustrated in Figure 10. Future research could focus on enhancing the controller by incorporating speed control. This would enable the vessel to align with the defined track more rapidly in a shorter reaction distance, as the current study is limited to only considering heading control.

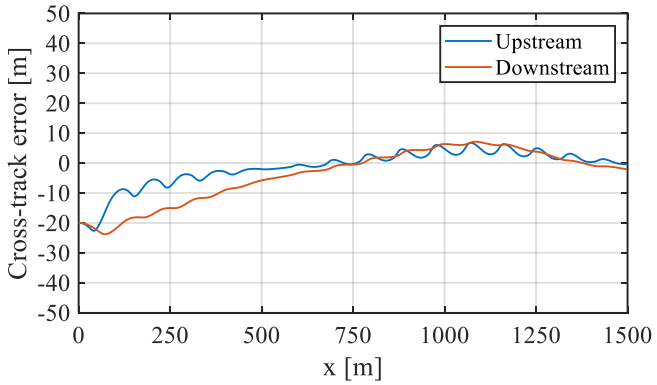

Figure 10: CROSS-TRACK ERROR RESULT.

4.4. Steering simulation at waterway confluence

Navigating a vessel through a waterway confluence or a "T-junction" poses unique challenges due to the need for proactive decision-making. Consequently, to facilitate increased reaction time, the vessel's operational speed was reduced from 150 rpm to 100 rpm.

To successfully execute a sharp turn, the vessel must initiate its manoeuvre well in advance. In this scenario, an advance distance of 2.5 times the vessel's length (L) was adopted, based on the results from the turning test in Figure 4. Selecting an

Copyright © 2024 by ASME

appropriate turn radius is critical for ensuring safety, considering varying environmental conditions such as current and potential unforeseen events. Furthermore, several internal factors, such as the vessel's maximum rudder angle, length, and speed, are pivotal in determining the feasible turn radius. Figure 11 presents the trajectory tracking results for the IWV for different current directions. The results confirm that the controller can adjust the ship's heading effectively, enabling it to adhere to the desired path.

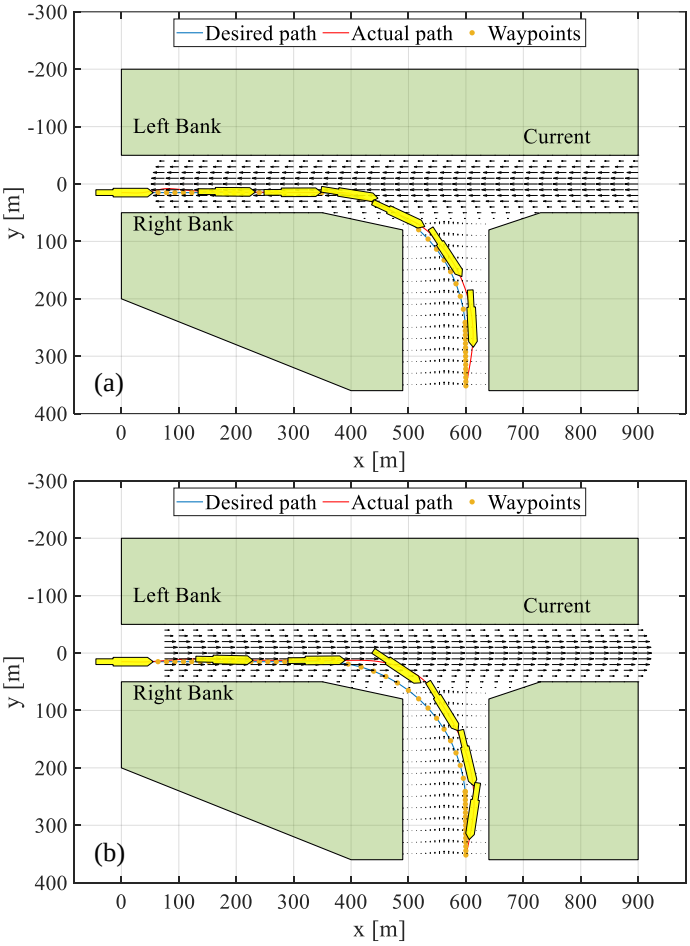

Figure 11: SIMULATION RESULTS FROM TURNING TRAJECTORY SIMULATIONS: (a) UPSTREAM CURRENT, AND (b) DOWNSTREAM CURRENT.

The results in Figure 11 show that the current assists in the vessel's turning manoeuvres for upstream conditions, effectively reducing the tracking errors. On the contrary, sailing downstream is more challenging, as the vessel tends to drift with the current, leading to increased tracking errors. These results showcase the limitations of using a PID controller in such complex manoeuvring scenarios, highlighting the need for more sophisticated model-based control strategies. Additionally, the insufficient steering force due to downstream sailing may also have contributed to the large course deviation. In that case, a simultaneous control of the vessel's speed could enhance the tracking performance; this is a topic for further investigation.

5. CONCLUSIONS

To develop voyage planning systems for autonomous IWVs, manoeuvring and control design are critical factors which must be considered. This study presents an enhanced control design, integrating a modified manoeuvring model that encapsulates the physical characteristics of inland waterways. The operational scenarios included typical conditions encountered by IWVs, such as navigating through river bends and waterway confluences.

The proposed model was verified using hydrodynamic coefficients derived from experimental results of a pusher-barge system in shallow water. The 20° and 35° turns results show good agreement with existing literature data, suggesting that the manoeuvring model accurately captures the steering behaviour of the pusher-barge model. Future studies will extend this investigation to various types of vessels, such as self-propelled barges or tankers, utilising available experimental data.

The results of control simulations showcase that the proposed heading control scheme can effectively handle the vessel's direction to follow the predefined waypoints under complex influence of riverbanks and currents. Navigating through a confluence is the most challenging scenario, requiring the vessel to execute a tight manoeuvre with a large angle. Consequently, the selection of an appropriate turn radius and waypoint generation considered the ship's advance distance in a proactive manner. The results showed that the vessel can effectively reduce tracking errors by leveraging upcoming currents. However, the observed course drifting and offset in downstream currents highlight the need for more advanced methods, such as model-based control, complemented by speed adjustments.

This study focused solely on waterways with rectangular-shaped cross-sections. Future research should encompass trapezoidal and even irregularly shaped cross-sections with varying water depths to more accurately represent the characteristics of natural rivers. In such conditions, the safety margins to banks, particularly to avoid shallow water, must be carefully assessed. Additionally, an operational analysis of the ships' energy performance is essential to evaluate the sustainability of these autonomous vessels. This would involve a comprehensive analysis encompassing ship hydrodynamics, energy systems, manoeuvring, and advanced routing algorithms. The model developed in the study will serve as a foundational tool for analysing these aspects.

ACKNOWLEDGEMENTS

This project has received funding from the European Union's EU Framework Programme for Research and Innovation Horizon 2020 under Grant Agreement No. 955768 (ETN AUTOBarge). Project website: https://etn-autobarge.eu/.

Copyright © 2024 by ASME

REFERENCES

[1] European Commission, 2023, “Freight transport statistics - modal split,” from https://ec.europa.eu/eurostat/statistics-explained/index.php?title=Freight_transport_statistics_-_modal_split.

[2] European Commission, 2020, “AUTOBarge: European training and research network on autonomous barges for smart inland shipping,” from https://etn-autobarge.eu/.

[3] Zhang C, Ringsberg J.W, Thies F., 2023. “Development of a ship performance model for power estimation of inland waterway vessels,” Ocean Engineering. 287,115731.

[4] Christodoulou A, Christidis P, Bisselink B., 2020. “Forecasting the impacts of climate change on inland waterways,” Transportation Research Part D: Transport and Environment. 82,102159.

[5] Xing S, Xinping Y, Bing W, Xin S., 2013. “Analysis of the operational energy efficiency for inland river ships,” Transportation Research Part D: Transport and Environment. 22, 34-39

[6] Koh, K., & Yasukawa, H., 2012. “Comparison study of a pusher–barge system in shallow water, medium shallow water and deep-water conditions,” Ocean Engineering, 46, 9–17

[7] Yoshimura, Y., 1986. “Mathematical model for the manoeuvring ship motion in shallow water,” Journal of the Kansai Society of Naval Architects (200).

[8] Zou, L., & Larsson, L., 2013. “Computational fluid dynamics (CFD) prediction of bank effects including verification and validation,” Journal of Marine Science and Technology, 18, 310–323.

[9] Liu J, Hekkenberg R, Rotteveel E, Hopman H., 2015. “Literature review on evaluation and prediction methods of inland vessel manoeuvrability,” Ocean Engineering. 106, 458-71.

[10] Zhang, C., Ma, Y., Thies, F., Ringsberg, J.W., Xing, Y., 2023. “Towards autonomous inland shipping: a manoeuvring model in confined waterways,” Accepted to be published in Ships and Offshore Structures.

[11] Ogawa A, Kasai H., 1978. “On the mathematical model of manoeuvring motion of ships,” International shipbuilding progress. 25, 306-319.

[12] Millward A., 1989. “The effect of water depth on hull form factor,” International shipbuilding progress.36.

[13] Vantorre M, Delefortrie G, Eloot K, Laforce E., 2003. “Experimental investigation of ship-bank interaction forces”.

[14] Ellis, George., 2012. Control system design guide: using your computer to understand and diagnose feedback controllers. Butterworth-Heinemann.

[15] Fossen, Thor I., 2011. Handbook of marine craft hydrodynamics and motion control. John Wiley & Sons.

[16] Duan, J.G., 2004. “Simulation of flow and mass dispersion in meandering channels,” Journal of Hydraulic Engineering, 130, 964-976.

Copyright © 2024 by ASME